INVOTEK
Jurnal Inovasi Vokasional dan Teknologi
http://invotek.ppj.unp.ac.id/index.php/invotek

Vol. 24, No. 2, June 2024
ISSN: 1411 – 3411 (p)
ISSN: 2549 – 9815 (e)

Design and Implementation MPPT Improved Whale Optimization Algorithm to Overcome Partial Shading Condition on Solar Panel

Muhammad Nizar Habibi[1] *, Rifqi Noviantono Prakoso[1], Ahmad Firyal Adila[1], Moh. Zaenal Efendi[1], Novie Ayub Windarko[1], Rachma Prilian Eviningsih[1]

[1] Department of Electrical Engineering, Politeknik Elektronika Negeri Surabaya
Jl. Raya ITS, Keputih, Kecamatan Sukolilo, Surabaya, Indonesia-60111

**Corresponding author: nizar@pens.ac.id*
Doi: https://doi.org/10.24036/invotek.v24i2.1219

Abstract

Solar energy is a type of renewable energy whose capacity is tremendous and fast in increasing its capacity so that it can be used for energy sustainability in the future. Solar panels are the only devices that can be used to utilize solar energy. Maximum Power Point Tracking (MPPT) is a method to maximize the power generated by solar panels. However, the problem with solar panels is the condition of partial shading, this occurs due to something blocking the rate of solar irradiation to the solar panel. The result is that there are 2 or more maximum power points from solar panels, the highest power is the Global Maximum Power Point (GMPP) and the other is the Local Maximum Power Point (LMPP). This partial shading condition cannot use conventional MPPT methods due to the complexity of finding GMPP. So, MPPT optimization method is needed, one of which is the Improved Whale Optimization Algorithm (IWOA). IWOA is a development of the Whale Optimization Algorithm (WOA) by applying the Sine-Tent-Cosine Map for the first time the algorithm works to be more effective in the initialization process of the algorithm population and can ensure a more uniform distribution of population distribution throughout the search space. IWOA will be applied to the MPPT system to achieve the GMPP of the solar panel under partial shading conditions.

Keywords: Solar Panel, MPPT, IWOA, Partial Shading Condition.

1. Introduction

Renewable energy is an energy that always exists in nature and is unlimited. Renewable energy possesses significant potential and demonstrates a rapid rate of growth in its energy production capabilities, so it can ensure energy sustainability in the future [1]. One example of renewable energy is solar energy. Solar energy has an energy potential of 207.8 GWp in Indonesia [2], with this much potential, there are many opportunities to utilize solar energy. One of the devices that can be used to utilize solar energy is solar panels [3]. The performance of solar panels is highly dependent on how much sunlight intensity and temperature received by solar panels [4]. However, the intensity of sunlight and temperature fluctuate, so the energy conversion produced by solar panels is not maximized [5].

Maximum Power Point Tracking (MPPT) is a method that can maximize the energy produced by solar panels [6]. MPPT can not only increase the power generated by solar panels, but MPPT can also increase the operating life of solar panels [7]. Currently, many researchers are developing MPPT methods to find the maximum power from solar panels. Starting from conventional methods such as Perturb and Observe (P&O) [8], Incremental Conductance (InC) [9], and Look-Up Table-Based MPPT (LTB MPPT) [10]. In addition to conventional methods, MPPT is also developed in the realm of intelligent control methods such as Artificial Neural Network (ANN) [11], and Fuzzy Logic Controller (FLC) [12]. Another problem that arises in the application of renewable energy using solar panels is partial shading conditions. Partial shading conditions are conditions where some solar panels on a PV array do not receive the same intensity of sunlight because they are partially obscured by an object [13]. So that it will result in the power generated by MPPT being low. In partial shading conditions, two types

P-ISSN: 1411-3414
E-ISSN: 2549-9815

of power will appear on solar panels, namely Global Maximum Power Point (GMPP) and Local Maximum Power Point (LMPP). This condition requires a special method to be able to map the correct position of the GMPP of the solar panel. One of the MPPT methods used is the optimization type method. Optimization algorithms improve all aspects of MPPT such as accuracy, efficiency, tracking speed, cost, complexity, and flexibility. Population variables are selected to adjust the value of the duty cycle which has an impact on changes in voltage and current to find GMPP on solar panels under partial shading conditions. Examples of optimization algorithms include Particle Swarm Optimization (PSO) [14], Differential Evolution (DE) [15], Grey Wolf Optimization (GWO) [16], Mountaineering Team-Based Optimization (MTBO) [17] and Whale Optimization Algorithm (WOA) [18].

In 2016, Mirjalili and Lewis [19] introduced Whale Oprimization Algorithm inspired by the stunning hunting behavior of humpback whales in the ocean. By the end of March 2023, WOA already have 7410 citations. This exponential growth shows the popularity and impact of this algorithm. Simple but powerful search mechanisms for finding the optimal solution with high speed are the main power of WOA [20]. However, WOA faces challenges such as slow convergence rate and limited global search efficiency [18]. So improvements or improvisations are needed from the optimization algorithms that have been developed. One of the optimization methods that has been further developed is the Improved Whale Optimization Algorithm (IWOA) [18]. IWOA enhances WOA by incorporating the Sine-Tent-Cosine Map during the initial implementation of the algorithm, which improves the initialization of the algorithm's population and ensures a more balanced distribution of populations throughout the search space. The original WOA creates the initial population in a random manner, which might lead to an uneven distribution of individuals across the potential solution space. This method may restrict The algorithm's ability to explore the search space, impacting its overall effectiveness in identifying optimal solutions. By applying the Sine-Tent-Cosine Map it hopes that the MPPT convergence time can be reduced. In this research, IWOA will be applied to the MPPT system for partial shading conditions on solar panels. The algorithm will control the output duty cycle value that will be sent to the power converter to get the GMPP value of the solar panel.

1.1 Photovoltaic

Solar panels are the main component of the MPPT system, as the main purpose of MPPT is to increase the energy conversion efficiency of solar panels. Figure 1 is the equivalent circuit of the solar panel. Based on Figure 1, the current equation that can be generated by the solar panel is shown in Equation (1). I_{pv} and V_{pv} are the current and voltage generated by the solar panel, I_s is the saturation current and Iph is the current generated by the solar panel when exposed to solar irradiation. n is the diode quality factor, R_{sh} and R_s are the parallel and series resistor values on the solar panel. Figure 1 shows the equivalent circuit of a solar panel.

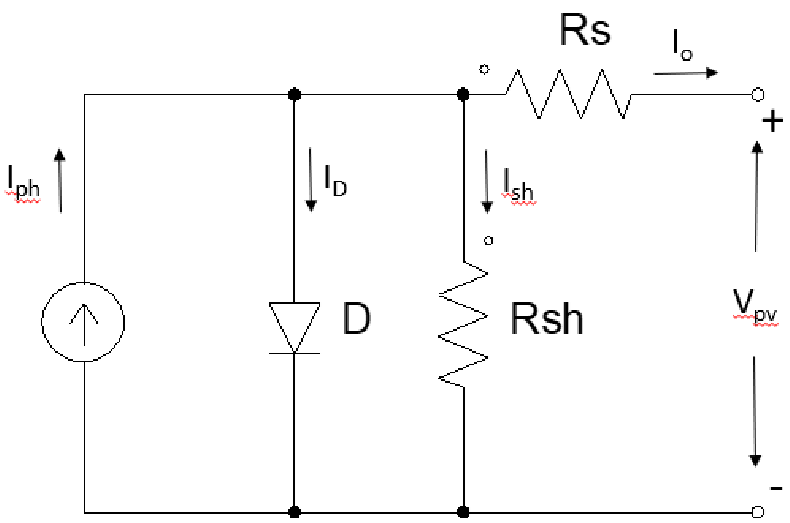

Figure 1. Equivalent Circuit of Solar Panel

The current that flows in the solar panel (I_{pv})

P-ISSN: 1411-3414
E-ISSN: 2549-9815

$$I_{pv} = I_{ph} - I_s \left(e^{\frac{V_{pv} + I_{pv} R_S}{n N_S V_t}} - 1 \right) - \frac{V_{pv} + I_{pv} R_S}{R_{sh}} \quad (1)$$

The I_{ph} current is completely dependent on solar irradiation and can be calculated using Equation (2). I_{sc} is the short-circuit current value of the solar panel, k_i is the short-circuit current temperature coefficient, G is the solar irradiation value and T_r is the temperature of the solar cell.

$$I_{ph} = \frac{G}{1000} \left(I_{sc} + k_i (T - T_r) \right) \quad (2)$$

1.2 Partial Shading Condition

PV Array is a system consisting of solar panel modules connected in series or parallel so that it will produce power which is an accumulation of the many solar panels connected in the PV array. Figure 2a is an illustration of a shadowed solar panel configuration, with the positioning of the "shadowed module" determined randomly. This will eliminate the power generated by the other solar panels. The shape of the curve generated by each solar panel module is shown in Figure 2b. When the solar panel is operating under the Ia condition, the partially shaded solar panel will be forced to operate in the reversed bias region, so it will have the properties of a load instead of a source.

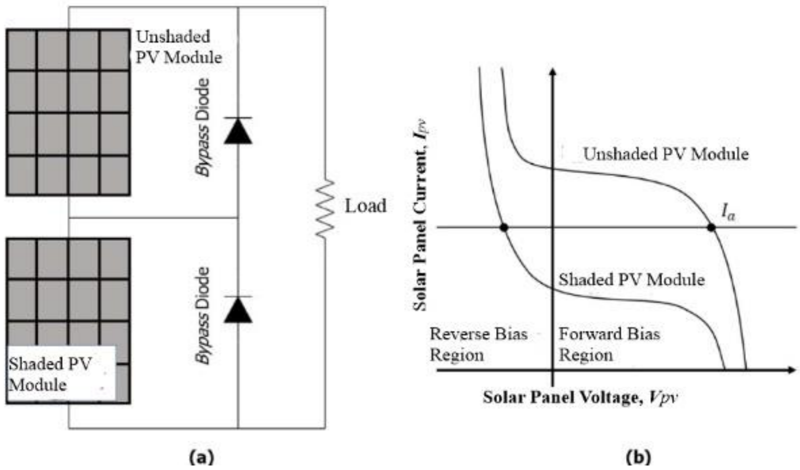

Figure 2. a) PV Array Configuration in Partially Shaded Conditions, b) PV Modul Characteristics

The phenomenon will cause power dissipation to heat which can result in damage to the shadowed solar panel module, so a bypass diode is installed to avoid both phenomena [21] as shown in Figure 2a.

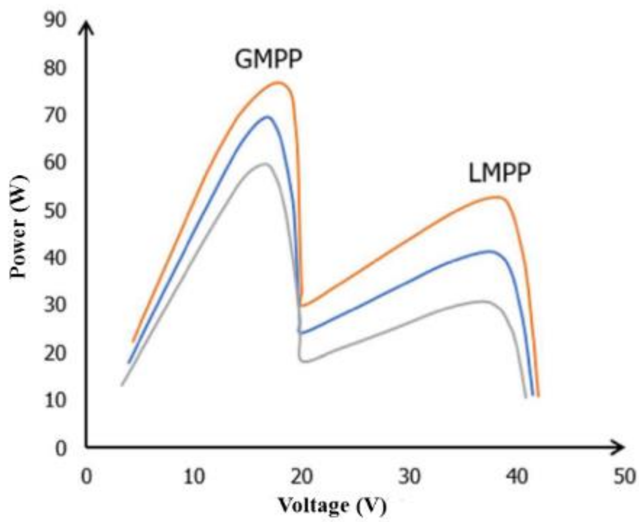

Figure 3. Solar Panel P-V Characteristics in Shaded Conditions

P-ISSN: 1411-3414
E-ISSN: 2549-9815

When exposed to solar radiation, the diode is reversed-biased. When there is partial shading on the solar panel, the bypass diode is forward biased and the current passes through the diode. As a result of the bypass diode, several Maximum Power Point (MPP) curves appear in the solar panel characteristic curve. The curve with the highest peak is called the Global Maximum Power Point (GMPP) and the curve with the next highest peak is the Local Maximum Power Point (LMPP) as shown in Figure 3. For partially shaded conditions, this paper is simplified by assuming different radiation on each panel. So, the definition of partial shading is the difference in radiation on each solar panel. The effect on the P-V characteristics is the same as partial shading on a solar panel.

1.3 Improved Whale Optimization Algorithm (IWOA)

The Whale Optimization Algorithm (WOA) draws its inspiration from the hunting strategies employed by whales. Key behaviors observed during whale hunting include encircling their prey, executing bubble-net attacks, and actively searching for prey. The WOA mathematically models these three predatory behaviors in the following manner.

1.3.1 Encircling Prey

During this phase, the WOA imitates the behavior of whales hunting for prey, successfully locating and encircling it. The prey is considered the best solution within the existing population. The main goal of this phase is to improve the search process's efficiency, focusing on identifying potential optimal solutions. The following mathematical formula can be used to describe this behavior:

$$X(t+1) = X - A.D_1 \tag{3}$$

$$D_1 = |C.X - X(t)| \tag{4}$$

In this model, t denotes the current iteration, and $X(t+1)$ refers to the subsequent search position. $X(t)$ represents the position at the current iteration, while $X*$ signifies the optimal target position for that iteration. The distance between the whale and the prey at $X(t)$ in the current iteration is denoted as D_1.

1.3.2 Bubble-Net Attacking

The bubble-net attack phase illustrates the behavior of a cluster of whales that rotates upward as they feed. During this phase, the whale makes its way toward the predicted location of its prey by tracing a spiral route. This behavior can be mathematically described using the following formula:

$$X(t+1) = D_2.e^{bl}.\cos\cos(2\pi l) + X \tag{5}$$

$$D_2 = |X - X(t)| \tag{6}$$

Where, D_2 represents the current distance between the whale and its prey, which is defined as the optimal solution, the mathematical model of a spiral path is formed by e^{bl} and $cos(2\pi l)$, with b functioning as the constant forming the spiral and l becoming a random number in [−1, 1].

1.3.3 Searching Prey

The prey exploration phase represents a comprehensive search strategy within the Whale Optimization Algorithm (WOA) aimed at discovering new potential target regions within the solution space. During this phase, the whale randomly chooses a search target and subsequently adjusts its current position in relation to that target. This behavior can be articulated using the following formula:

$$X(t+1) = X_{rand}(t) - A.D_3 \tag{7}$$

$$D_3 = |C.X_{rand}(t) - X(t)| \tag{8}$$

1.3.4 Improved WOA

IWOA integrates the operators of the Whale Optimization Algorithm (WOA) with the mutation operator from Differential Evolution (DE) to enhance the balance between exploration and exploitation in WOA. When rand < λ the exploration part changes the individuals, λ is adjusted using the following formula:

$$\lambda = 1 - \frac{t}{t_{max}} \tag{9}$$

P-ISSN: 1411-3414
E-ISSN: 2549-9815

In this context, t represents the present generation, while tmax indicates the upper limit of generations. As outlined in Equation (9), the parameter k decreased progressively from 1 to 0 over time. The exploitation aspect of the Improved Whale Optimization Algorithm (IWOA) is comparable to that of the Whale Optimization Algorithm (WOA). In contrast, IWOA utilizes an elitism technique, setting it apart from WOA.. Namely, the new position for ith individual in the next generation is the fitter one between parent X_i and off-spring U_i. It is important to note that, solutions should consider boundary constraints. If these constraints are violated, the repairing rule is applied according to Equation (10).

$$X_i(j) = \begin{cases} \delta_j + rndreal(0,1) \times (\mu_j - \delta_j)\ if\ X_i(j) < \delta_j \\ \mu_j - rndreal(0,1) \times (\mu_j - \delta_j)\ if\ X_i(j) < \mu_j \end{cases} \tag{10}$$

Where, μ_j and δ_j are the upper bound and lower bound of the *j*th dimension respectively. $X_i(j)$ is the *j*th dimension of *i*th solution, rndreal (0, 1) is a random number between 0 and 1.

2. Experimental Method

The experiment is carried out using PSIM simulation software, which models the photovoltaic (PV) system to reflect the characteristics of a real-world PV setup. A Buck Converter is integrated into the simulation, serving as the connection between the PV and the load. The PV generates power, while the Buck Converter manages this power output through adjustments to the duty cycle percentage. An algorithm facilitates automatic control of the duty cycle, and the performance of the Improved Whale Optimization Algorithm (IWOA) will be demonstrated by the PV's power output, particularly under conditions of partial shading. Figure 4 provides a block diagram of the MPPT system.

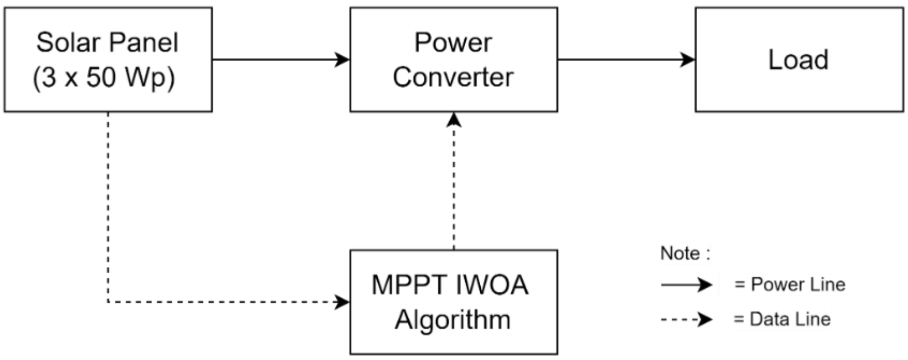

Figure 4. Block Diagram MPPT IWOA System

The MPPT system uses three 50 Wp Solar panels that are connected in series so the total power reaches 150 Wp. The data that are inputted to the Algorithm are the Input voltage and Input current, from those data algorithm will process the power value till the algorithm finds the best power value. Table 1 shows the solar panel characteristics that are taken from the real PV.

Table 1. PV Module Parameters

Parameters	ST Solar
P_{max} (W)	50
V_{mp} (V)	17.8
I_{mp} (A)	2.81
V_{oc} (V)	21.89
I_{oc} (A)	3.03

Where, V_{mp} and I_{mp} are the maximum voltage and current from the solar panel that is still generating power, while V_{oc} and I_{oc} are the voltage in an open circuit and current in a short circuit. Another important part of the MPPT System is the Power Converter, the power converter that is used in this experiment is the Buck Converter. Buck Converter component value is customized as per the value of PV. Figure 5 shows the Buck Converter Schematic Design.

P-ISSN: 1411-3414
E-ISSN: 2549-9815

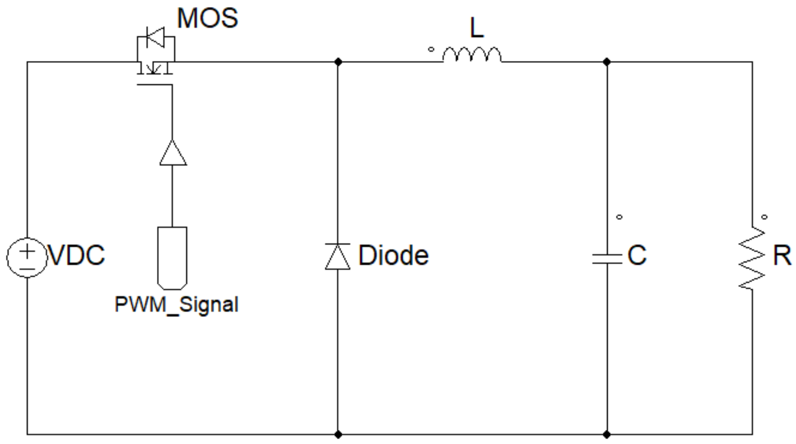

Figure 5. Buck Converter Design

The buck converter serves as the intermediary between the photovoltaic (PV) array and the load. By adjusting the duty cycle of the buck converter, the load impedance can be modified as perceived from the PV array perspective. This adjustment facilitates the buck converter in optimizing the PV operating point at the maximum power point (GMPP) impedance. The Buck Converter can be formulated using Equations (11)–(15).

$$D = \frac{t_{on}}{T_s} \tag{11}$$

$$V_o = D \times V_i \tag{12}$$

$$C = \frac{1 - D}{8L\left(\frac{\Delta V_O}{V_O}\right)f^2} \tag{13}$$

$$L = \left(\frac{V_i - V_o}{\Delta i_L f}\right) D \tag{14}$$

$$L_{min} = \frac{(1-D)R}{2f} \tag{15}$$

Where, D is the duty cycle, t_{on} is PWM signal duration to turn on buck converter switch, T_s is switching period, V_o and V_i are the input and output voltages, C and L are the capacitor and inductor, respectively, f is the switching frequency, L_{min} is the minimum inductance needed for continuous current operation, R is load resistance, ΔV_o is the load ripple voltage, and Δi_L is the inductor ripple current. Table 2 shows the Buck Converter components value that will be used in this simulation.

Table 2. Buck Converter Parameters

Parameters	ST Solar
V_{in} (V)	41.8
V_o (V)	14.4
f_s (kHz)	40
C (µF)	315
L (µH)	180

3. Result and Discussion

To evaluate the performance of IWOA, the performances were compared to the performances of two other algorithms, WOA and MTBO Algorithm. 5 irradiance patterns were used to see the performances of each algorithm. In this MPPT simulation, 1 uniform irradiance pattern is used and 4 partial shading irradiance patterns are used to evaluate the algorithms. In this MPPT System, Buck Converter is used to reduce the voltage that is well matched with the load.

P-ISSN: 1411-3414
E-ISSN: 2549-9815

Table 3. Irradiance Value in Three Different PV

Irradiance Pattern	PV 1 (W/m^2)	PV 2 (W/m^2)	PV 3 (W/m^2)
Pattern 1	1000	1000	1000
Pattern 2	1000	850	400
Pattern 3	800	1000	450
Pattern 4	400	650	1000
Pattern 5	250	500	1000

The Table 3 shows each irradiance value in three different PV. Pattern 1 will show uniform irradiance that has only one GMPP. Patterns 2-5 will show three different peaks that are caused by partial shading. The three peaks have different values caused by different irradiance values in each PV that will cause three different peaks. Figure 6 shows the P-V characteristics of uniform and partially shaded PV.

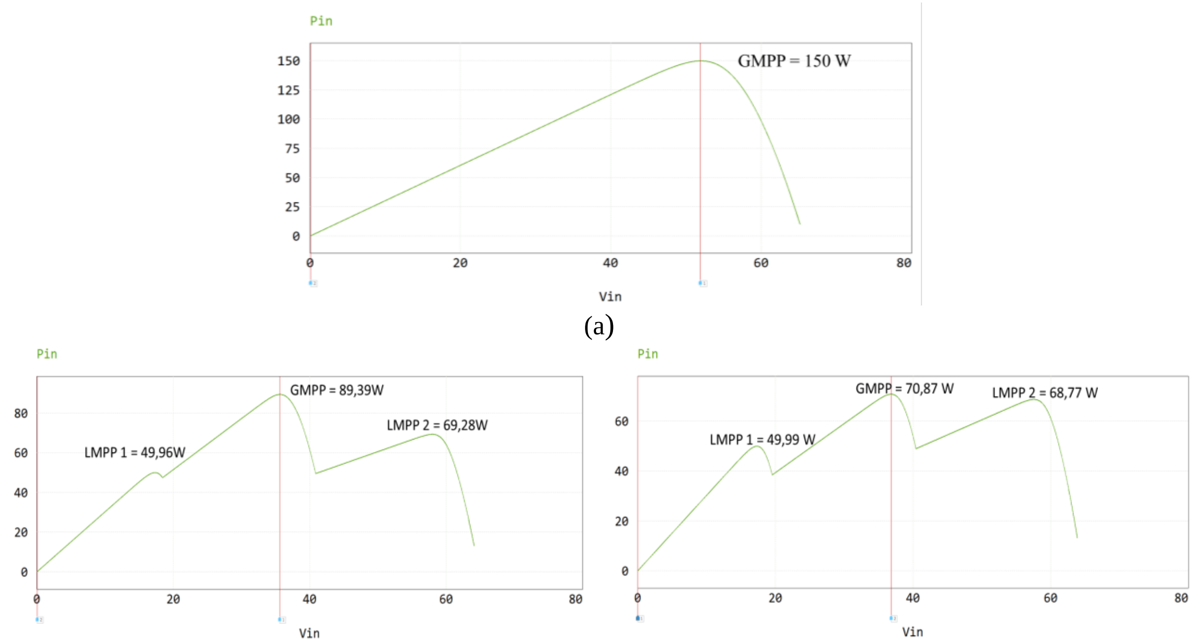

(a)

(b) (c)

Figure 6. P-V Characteristics Curve (a) Pattern 1 (b) Pattern 2 (c) Pattern 4

From Figure 6 we can see that partial shadings will affect the power generated from the PV. In pattern (a) the maximum power value is 150 W and the reason is caused by all three PVs produce a maximum power of 50 Wp with a total value of 150 Wp, in pattern (b) the GMPP in the middle with the value of 89.39 W. The differences in the peak position can determine whether the algorithm is capable enough to perform in each irradiance pattern or different GMPP peak positions and whether the algorithm can escape from the LMPP peak. Figure 7 shows the performance of IWOA on pattern 1.

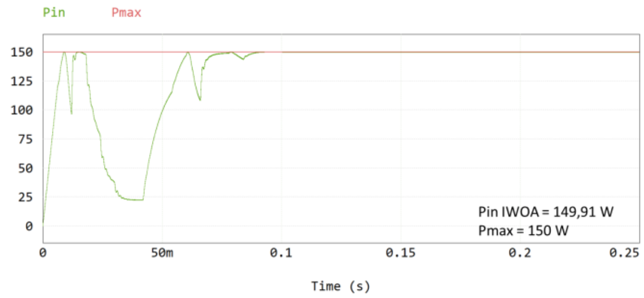

Figure 7. P-Time Simulation Results IWOA Pattern 1

From Figure 7 we can see that IWOA can reach the GMPP shown by the value that IWOA obtained is 149.91 W with the power target of 150 W. This makes IWOA in this pattern have an accuracy

P-ISSN: 1411-3414
E-ISSN: 2549-9815

of 99.94 %. From Figure 6 we can see that pattern 1 only has 1 GMPP, and as a result, we can say that IWOA can reach GMPP if there is only one peak. A lot of algorithms can reach GMPP if there is only one peak, so the real test is whether IWOA can also overcome partial shading. Figure 8 shows the results of IWOA on patterns 2 until 5.

From Figure 8 we can see the performance of IWOA in partial shading conditions. In pattern 3, IWOA accuracy can reach 99.68 % with power generated from IWOA 84.75 W with a power target of 85.02 W. Still, in pattern 2, IWOA accuracy only reached 97.30% IWOA generated power of 86.98 W with power target of 89.39 W. This show that IWOA overall didn't get stuck on LMPP but on some irradiance condition, IWOA cannot reach an accuracy of 99% or above. Another advantage of IWOA is the tracking speed, from the simulation results we can see that IWOA has a high-speed tracking time with an average tracking time of 0.18 s. To see the performance of IWOA, we need to compare the simulation results of IWOA to another algorithm, and in this experiment, IWOA will be compared to WOA and MTBO. Figure 8 Shows the P-Time simulation result of IWOA compared to WOA and MTBO on pattern 2.

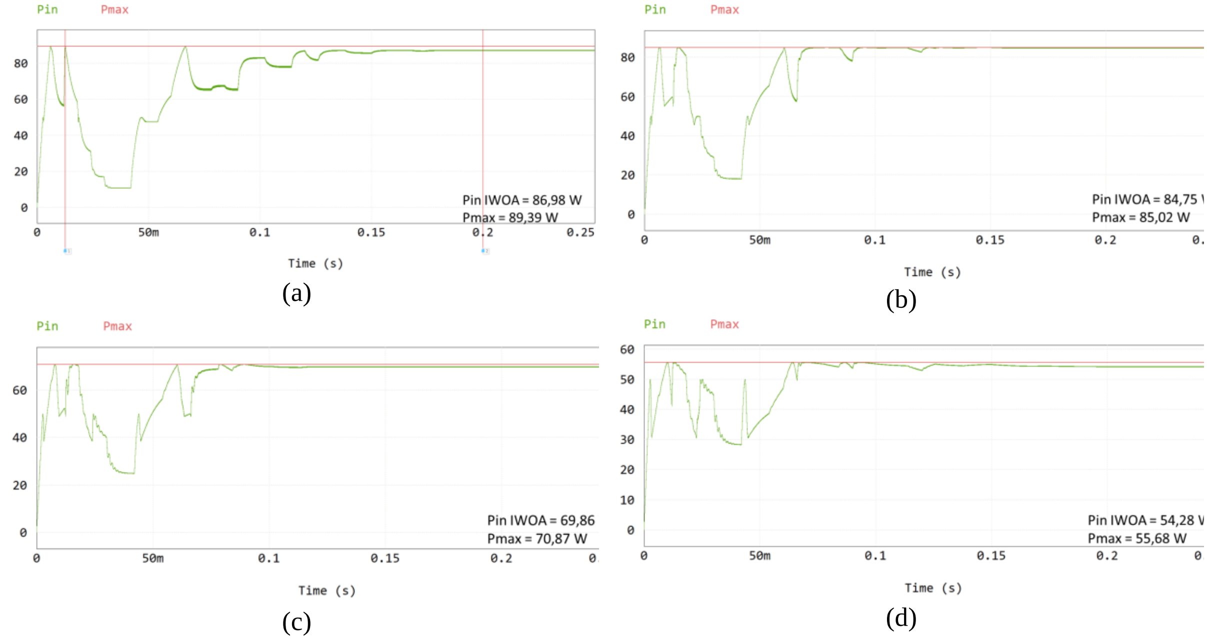

Figure 8. P-Time Simulation Results IWOA Pattern (a) Two (b) Three (c) Four (d) Five

Figure 9 illustrates the simulation outcomes for pattern 1, comparing the performance of IWOA, WOA, and MTBO. Given that this pattern exhibits a single peak, the results indicate that all three algorithms perform exceptionally well, with accuracy rates exceeding 99% for each. Additionally, it is noteworthy that IWOA demonstrated a shorter tracking time to achieve a steady state compared to both WOA and MTBO. Specifically, IWOA required 0.15 seconds to reach a steady state, whereas MTBO took 0.8 seconds and WOA required 0.2 seconds.

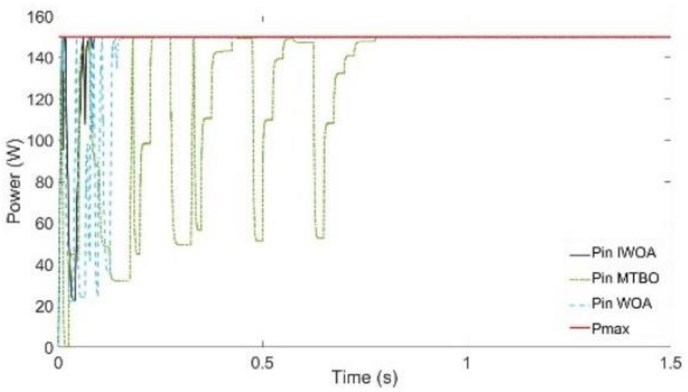

Figure 9. P-Time Simulation Results Pattern 1

P-ISSN: 1411-3414
E-ISSN: 2549-9815

Figure 10 illustrates the P-Time simulation outcomes for IWOA, WOA, and MTBO. The IWOA is represented by a black line, MTBO by a green line, WOA by a blue line, and Pmax by a red line. The simulation results indicate that for patterns 2 and 3, IWOA outperformed both WOA and MTBO.

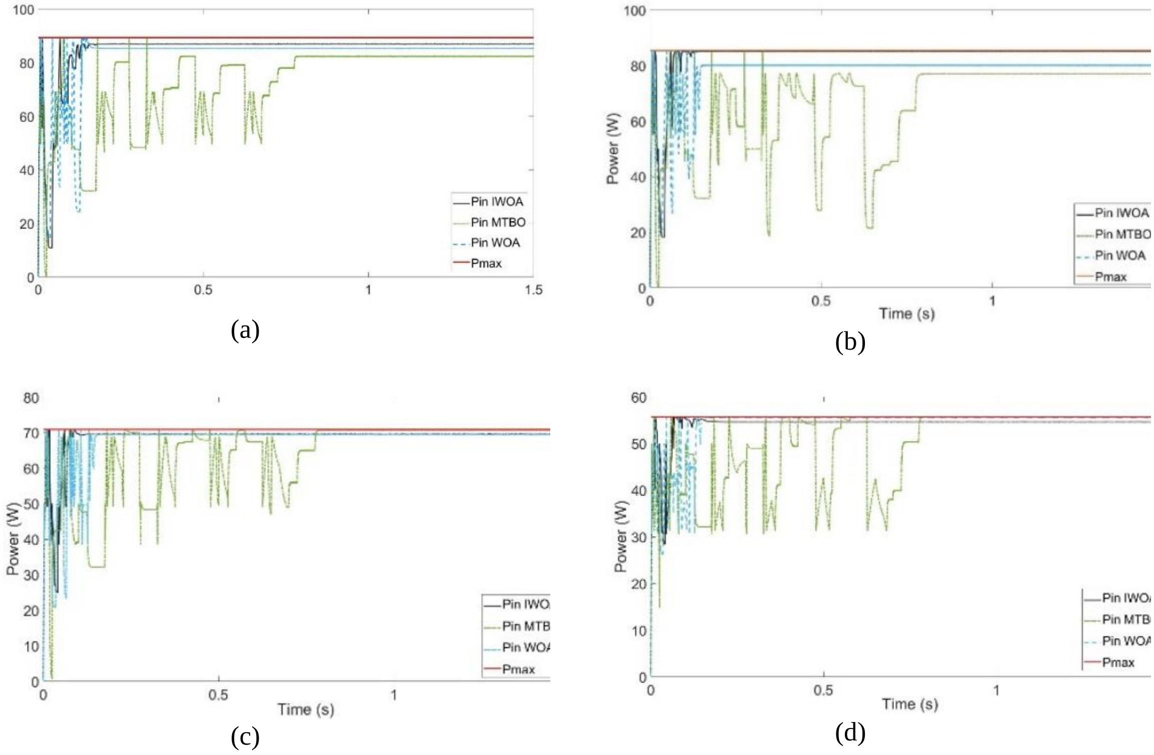

Figure 10. P-Time Simulation Results Pattern (a) Pattern 2 (b) Pattern 3 (c) Pattern 4 (d) Pattern 5

Specifically, IWOA achieved an accuracy of 97.30% for pattern 2 and 99.68% for pattern 3. In contrast, WOA recorded accuracies of 95.42% and 94.33% for patterns 2 and 3, respectively, while MTBO achieved 92.05% and 90.63%. Additionally, in terms of tracking time, both IWOA and WOA demonstrated superior performance compared to MTBO, with IWOA and WOA requiring 0.2 seconds to reach a steady state, whereas MTBO required 0.8 seconds. Meanwhile, for patterns 4 and 5, MTBO exhibited better performance than both IWOA and WOA, achieving accuracies exceeding 99%. In these patterns, IWOA recorded accuracies of 98.57% and 97.48%, while WOA achieved 97.79% and 99.83%. IWOA displayed a faster convergence speed, taking only 0.15 seconds to reach a steady state for pattern 4, compared to MTBO's 0.8 seconds and WOA's 0.2 seconds. For pattern 5, both IWOA and WOA reached a steady state in 0.2 seconds, while MTBO took 0.8 seconds. Overall, the results indicate that IWOA and MTBO excel in different irradiance patterns, with IWOA consistently demonstrating faster convergence speeds across all patterns due to MTBO needed to complete the number of total iterations and then show the simulation results. Table 4 shows the simulation results of all five patterns. Tracking oscillation from Table 4 are obtained from the amount of ripple in tracking state, from the p-time simulation results, it is seen that IWOA have rather less tracking ripple than WOA and MTBO. Sine-Tent-Cosine Map help reduced the search time for the optimal solution. The result shows that IWOA have a faster convergence time than WOA. The stability of the algorithm under partial shading conditions is based on the performance of tracking oscillation. Because on metaheuristic algorithm, there will be no change on optimal power obtained. Based on that, IWOA have a better stability rather than WOA and MTBO.

Table 4. Simulation Results

Pattern 1	Power Target (W)	Pin (W)	Tracking Efficiency (%)	Convergence Time (s)	Power Loss (W)	Tracking Oscillation
IWOA	150	149.91	99.94	0.15	0.09	small
WOA	150	149.26	99.50	0.2	0.74	varies

P-ISSN: 1411-3414
E-ISSN: 2549-9815

MTBO	150	149.97	99.98	0.8	0.03	varies
Pattern 2	Power Target (W)	Pin (W)	Tracking Efficiency (%)	Convergence Time (s)	Power Loss (W)	Tracking Oscillation
IWOA	89.39	86.98	97.30	0.2	2.41	small
WOA	89.39	85.30	95.42	0.2	4.09	varies
MTBO	89.39	82.29	92.05	0.8	7.1	varies
Pattern 3	Power Target (W)	Pin (W)	Tracking Efficiency (%)	Convergence Time (s)	Power Loss (W)	Tracking Oscillation
IWOA	85.02	84.75	99.68	0.2	0.27	small
WOA	85.02	80.20	94.33	0.2	4.82	varies
MTBO	85.02	77.06	90.63	0.8	7.96	varies
Pattern 4	Power Target (W)	Pin (W)	Tracking Efficiency (%)	Convergence Time (s)	Power Loss (W)	Tracking Oscillation
IWOA	70.87	69.86	98.57	0.15	1.01	small
WOA	70.87	69.31	97.79	0.2	1.56	varies
MTBO	70.87	70.70	99.76	0.8	0.17	varies
Pattern 5	Power Target (W)	Pin (W)	Tracking Efficiency (%)	Convergence Time (s)	Power Loss (W)	Tracking Oscillation
IWOA	55.68	54.28	97.48	0.2	1.4	small
WOA	55.68	55.59	99.83	0.2	0.09	varies
MTBO	55.68	55.64	99.92	0.8	0.04	varies

4. Conclusion

This experiment aims to see the performance of the Improved Whale Optimization Algorithm (IWOA) when implemented in MPPT partial shading problems. In this experiment, IWOA performance is compared to two other algorithms namely Whale Optimization Algorithm (WOA) and Mountaineering Team-Based Optimization (MTBO). The experiment is conducted by simulation using PSIM Software. Simulation results show that IWOA can compete with another algorithm in this problem, shown by the simulation results that IWOA in patterns 2 and 3 have better results than WOA and MTBO. But in Patterns 4 and 5, MTBO and WOA showed better results than IWOA. The advantage of IWOA is that this algorithm has a relatively faster tracking time than WOA and MTBO. The average tracking time of IWOA is 0.18 s while WOA is 0.2 s and MTBO 0.8 s. This shows that IWOA has a faster convergence time than the other algorithm.

References

[1] J. S. Setyono, F. H. Mardiansjah, and M. F. K. Astuti, "Potensi pengembangan energi baru dan energi terbarukan di kota semarang," *J. Riptek*, vol. 13, no. 2, pp. 177–186, 2019, doi: https://doi.org/10.35475/riptek.v13i2.68.

[2] F. Afif and A. Martin, "Tinjauan potensi Dan Kebijakan energi surya di Indonesia," *J. Engine Energi, Manufaktur, dan Mater.*, vol. 6, no. 1, pp. 43–52, 2022, doi: https://doi.org/10.30588/jeemm.v6i1.997.

[3] M. S. Al Amin, E. Emidiana, I. K. Pebrianti, and Y. Irwansi, "Penggunaan Panel Surya Sebagai Pembangkit Listrik Pada Alat Pengering Makanan," *J. Ampere*, vol. 7, no. 1, pp. 15–21, 2022, doi: https://doi.org/10.31851/ampere.v7i1.7703.

[4] S. W. Putri, G. Marausna, and E. E. Prasetiyo, "Analisis Pengaruh Intensitas Cahaya Matahari Terhadap Daya Keluaran Pada Panel Surya," *Tek. STTKD J. Tek. Elektron. Engine*, vol. 8, no. 1, pp. 29–37, 2022, doi: https://doi.org/10.56521/teknika.v8i1.442.

[5] D. A. K. Wida, K. Sumaja, and P. P. H. Wiguna, "Analisis Hubungan Intensitas Radiasi Dan Lama Penyinaran Matahari Dengan Parameter Cuaca Di Stasiun Meteorologi Ngurah Rai Serta Pengaruhnya Terhadap Potensi Pembangkit Listrik Tenaga Surya Di Bali Selatan," *Meteo Ngurah*

P-ISSN: 1411-3414
E-ISSN: 2549-9815

Rai, vol. 5, no. 1, pp. 1–7, 2019.

[6] B.-R. Peng, K.-C. Ho, and Y.-H. Liu, "A novel and fast MPPT method suitable for both fast changing and partially shaded conditions," *IEEE Trans. Ind. Electron.*, vol. 65, no. 4, pp. 3240–3251, 2017, doi: 10.1109/TIE.2017.2736484.

[7] S. Motahhir, A. El Ghzizal, S. Sebti, and A. Derouich, "Modeling of photovoltaic system with modified incremental conductance algorithm for fast changes of irradiance," *Int. J. Photoenergy*, vol. 2018, no. 1, p. 3286479, 2018, doi: https://doi.org/10.1155/2018/3286479.

[8] P. E. Broto and J. A. Hamonangan, "Review perbandingan teknik Maximum Power Point Tracker (MPPT) untuk sistem pengisian daya menggunakan sel surya," *J. Teknol. Dirgant.*, vol. 16, no. 2, 2018, doi: 10.30536/j.jtd.2018.v16.a2998.

[9] L. P. S. Raharja, R. P. Eviningsih, I. Ferdiansyah, and D. S. Yanaratri, "Penggunaan Daya Panel Surya Dengan MPPT Bisection Pada Proses Charging Baterai," *J. Teknol. Terpadu*, vol. 9, no. 1, pp. 24–33, 2021.

[10] X. Yue, D. Geng, Q. Chen, Y. Zheng, G. Gao, and L. Xu, "2-D lookup table based MPPT: Another choice of improving the generating capacity of a wave power system," *Renew. Energy*, vol. 179, pp. 625–640, 2021, doi: https://doi.org/10.1016/j.renene.2021.07.043.

[11] M. N. Habibi, M. S. W. Jati, N. A. Windarko, and A. Tjahjono, "Maximum Power Point Tracking Menggunakan Algoritma Artificial Neural Network Berbasis Arus Hubung Singkat Panel Surya," *J. Rekayasa Elektr.*, vol. 16, no. 2, 2020, doi: 10.17529/jre.v16i2.14860.

[12] U. Yilmaz, A. Kircay, and S. Borekci, "PV system fuzzy logic MPPT method and PI control as a charge controller," *Renew. Sustain. Energy Rev.*, vol. 81, pp. 994–1001, 2018, doi: https://doi.org/10.1016/j.rser.2017.08.048.

[13] V. Waghmare-Ujgare and M. D. Goudar, "Exploration of partial shading condition in photovoltaic array," in *2017 International Conference on Energy, Communication, Data Analytics and Soft Computing (ICECDS)*, 2017, pp. 931–936. doi: 10.1109/ICECDS.2017.8389572.

[14] W. Hayder, E. Ogliari, A. Dolara, A. Abid, M. Ben Hamed, and L. Sbita, "Improved PSO: a comparative study in MPPT algorithm for PV system control under partial shading conditions," *Energies*, vol. 13, no. 8, p. 2035, 2020, doi: https://doi.org/10.3390/en13082035.

[15] A. P. Firmanza, M. N. Habibi, N. A. Windarko, and D. S. Yanaratri, "Differential evolution-based mppt with dual mutation for pv array under partial shading condition," in *2020 10th Electrical Power, Electronics, Communications, Controls and Informatics Seminar (EECCIS)*, 2020, pp. 198–203. doi: 10.1109/EECCIS49483.2020.9263430.

[16] A. Tjahjono, D. O. Anggriawan, M. N. Habibi, and E. Prasetyono, "Modified grey wolf optimization for maximum power point tracking in photovoltaic system under partial shading conditions," *Int. J. Electr. Eng. Informatics*, vol. 12, no. 1, pp. 94–104, 2020, doi: 10.15676/ijeei.2020.12.1.8.

[17] R. N. Prakoso, M. Z. Efendi, and M. N. Habibi, "Design and Implementation Mountaineering Team-Based Optimization Algorithm for MPPT on Partial Shading Conditions," in *2024 International Electronics Symposium (IES)*, 2024, pp. 43–48. doi: 10.1109/IES63037.2024.10665787.

[18] Z. Liang, T. Shu, and Z. Ding, "A novel improved whale optimization algorithm for global optimization and engineering applications," *Mathematics*, vol. 12, no. 5, p. 636, 2024, doi: https://doi.org/10.3390/math12050636.

[19] S. Mirjalili and A. Lewis, "The whale optimization algorithm," *Adv. Eng. Softw.*, vol. 95, pp. 51–67, 2016, doi: https://doi.org/10.1016/j.advengsoft.2016.01.008.

[20] M. H. Nadimi-Shahraki, H. Zamani, Z. Asghari Varzaneh, and S. Mirjalili, "A systematic review

P-ISSN: 1411-3414
E-ISSN: 2549-9815

of the whale optimization algorithm: theoretical foundation, improvements, and hybridizations," *Arch. Comput. Methods Eng.*, vol. 30, no. 7, pp. 4113–4159, 2023, doi: 10.1007/s11831-023-09928-7.

[21] C. Olalla, C. Deline, and D. Maksimovic, "Performance of mismatched PV systems with submodule integrated converters," *IEEE J. Photovoltaics*, vol. 4, no. 1, pp. 396–404, 2013, doi: 10.1109/JPHOTOV.2013.2281878.